

Configuration Effect on LH Transition in Tohoku University Helicac

TAKAHASHI Hiromi, KITAJIMA Sumio, YOKOYAMA Masayuki¹, TANAKA Yutaka, UTOH Hiroyasu,
HASHIZUME Hidetoshi, SASAO Mamiko and TAKAYAMA Masakazu²

Department of Quantum Science and Energy Engineering, Tohoku University, Miyagi, 980-8579, Japan

¹National Institute for Fusion Science, Gifu, 509-5292, Japan

*²Department of Electronics and Information Systems, Akita Prefectural University,
Akita, 015-0055, Japan*

(Received: 9 December 2003 / Accepted: 29 July 2004)

Abstract

Electrode biasing experiments in three types of magnetic configuration were carried out to investigate the influence of poloidal ion viscosity on L-H transition in Tohoku University Helicac (TU-Helicac). Poloidal ion viscosity values estimated from experiments had local maxima at a poloidal Mach number $M_p \sim -2.4$, where plasmas showed negative differential resistance, in all configurations studied. However, the ion viscosity at the local maximum is dependent on the configuration. The ion poloidal viscosity was calculated based on neoclassical theory and it showed good agreement with that estimated from experiment. The results of calculations showed local maxima at $M_p \sim -2.4$ in all configurations, and indicated configuration dependence. These tendencies agreed with the experimental results.

Keywords:

plasma, helicac, stellarator, electrode, biasing, radial electric field, poloidal rotation, H mode, L-H transition, viscosity

1. Introduction

Although the H mode is widely observed in various tokamaks, such as ASDEX [1], DIII-D [2], TFTR [3], etc., there have been only a few reports in helical/stellarator devices, such as Wendelstein 7-AS [4] and CHS [5]. One of the characteristics of the H mode is poloidal rotation induced by a radial electric field. The shear poloidal rotation suppresses fluctuation levels in plasma and results in a decrease in anomalous transport coefficient. These phenomena were confirmed in both tokamaks and helical/stellarator devices. In TU-Helicac, the influence of a radial electric field on plasma parameters was investigated by electrode-biasing experiments. In both positive and negative biasing experiments, the improvement of plasma confinement was clearly observed when the radial electric field was formed [6-8].

The neoclassical theory points out the criterion of L-H transition from the viewpoint of ion viscosity. In this theory, the ion viscosity has a local maximum against the rotation velocity. When the driving force in poloidal direction exceeds a critical value, the poloidal rotation velocity increases rapidly and a plasma transits into the H mode. So far, various models for ion viscosity are proposed to explain L-H transition phenomena [9-11]. However, these models have not yet been examined in detail by experiment because it is difficult to

measure the ion orbit loss and the radial electric field with sufficient precision in both temporal and spatial resolution.

Motivated by the present state of the H mode study described above, we performed an electrode-biasing experiment under the active control of the electrode current, where the bifurcation phenomena with multiple solutions are degenerated. In the present study, the L-H transition with three types of magnetic configuration, which have different Fourier components, was studied experimentally to investigate the influence of poloidal ion viscosity in TU-Helicac. We report here that the critical driving force for the H mode transition is dependent on the configuration, and compare the experimental results with neoclassical theory where the Shaing model [12,13] is applied to ion viscosity.

2. Experimental setup

The TU-Helicac is a small helicac device of $n = 4$, where n is the toroidal period [14,15]. The helicac configurations are produced by three sets of coils: toroidal field coils, a center conductor coil, and vertical field coils. Various magnetic configurations can be formed easily by selecting ratios of coil currents, and Fourier components can be varied widely. The configuration parameters for typical cases of TU-Helicac are summarised in Table 1. The target plasma in biasing experiments is produced by alternative ohmic heating of 18.8

kHz. The vacuum vessel is filled with the fuelling gas He before discharge. Plasma parameters are measured using a Langmuir probe (triple probe) at toroidal angle $\phi = 0^\circ$ and a 6 mm microwave interferometer at $\phi = 90^\circ$. The hot cathode made of LaB₆, used as an electrode to form a radial electric field, is inserted horizontally from the low magnetic field side at $\phi = 270^\circ$. It is biased against the vacuum vessel by a *constant current* power supply. In this study, we attempted to control the poloidal driving force to clarify the role of ion viscosity for L-H transition. The poloidal driving force is the Lorentz force of $\mathbf{J} \times \mathbf{B}$. Thus, it can be changed continuously by the electrode current control. Figure 1 shows the magnetic surfaces and the position of the hot cathode in three types of configurations with magnetic axis R_{ax} located at (a) 7.7 cm, (b) 7.9 cm (standard configuration), and (c) 8.4 cm, respectively here the magnetic axis is defined in a poloidal cross section $\theta = 0^\circ$. They have similar profiles of rotational transform.

Table 1 The configuration parameters in four types of configuration.

R_{ax} (cm)	a (cm)	Well depth (%)	ϵ_{mn} ($r/R_0 = 0.05$; Boozer)		
			(0,1)	(1,0)	(1,1)
7.3	6.3	-0.99	-0.09	-0.051	-0.060
7.5	6.6	-0.11	-0.11	-0.049	-0.056
7.9	6.8	2.3	-0.13	-0.040	-0.051
8.4	6.2	4.1	-0.16	-0.039	-0.050

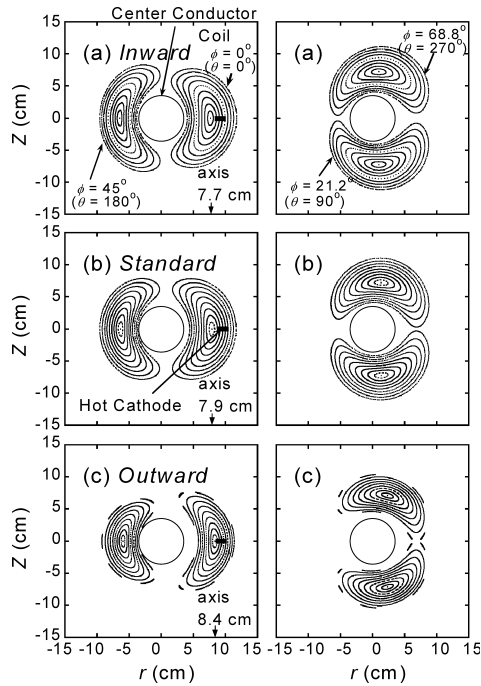


Fig. 1 The magnetic surfaces and the positions of the hot cathode in three types of configuration. The magnetic axes are located at (a) 7.7 cm, (b) 7.9 cm (standard configuration), and (c) 8.4 cm, respectively here θ stands for the poloidal angle around the Center Conductor Coil.

3. Experimental results

Typical time evolutions of electrode current I_E , bias voltage V_E and electron line density \hat{n}_e are shown in Fig. 2. Here, $T_e \approx 20$ eV, $n_e \approx 2 \times 10^{12}$ cm⁻³ at $\rho = 0.5$ and $B_0 \approx 0.3$ T in each configuration. I_E is controlled with the *constant current* power supply such that I_E is maintained at -4.2 A from $t = 0$ ms to 5 ms, and $-I_E$ is ramped down to 0 A from 5 ms to 10 ms. In each configuration, there is a region where $-V_E$ increases even though $-I_E$ decreases, indicating that the plasma shows negative differential resistance. In this region, various characteristics were observed, such as a decrease in plasma pressure, an increase in fluctuation level, etc. [16]. As shown in Fig. 3, I_E follows an *s-shape* curve against V_E , showing bifurcation.

The upper side of Fig. 4 shows the profiles of radial electric field E_r at the H mode (open circles), just before transition to the L mode (open diamonds) and at the L mode (open squares) in each configuration and the lower side of that shows time evolutions of E_r at different radial positions. Here, ρ is the averaged minor radius normalised by the averaged plasma radius a . The profiles of E_r show that the steeper gradient region shifts to the inside with $-I_E$ decreasing in each configuration. This indicated that E_r collapses from the outer to the inner region at the transition from H mode to

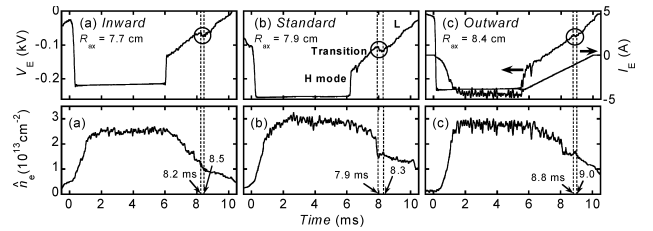


Fig. 2 Typical time evolutions of electrode current I_E , bias voltage V_E and electron line density \hat{n}_e for the configurations of (a) $R_{ax} = 7.7$ cm, (b) 7.9 cm, and (c) 8.4 cm. I_E is controlled with a constant current power supply so that I_E is maintained at -4.2 A during biasing time $t = 0$ ms and 5 ms, and $-I_E$ is ramped down to 0 A from 5 ms to 10 ms. The plasma shows negative differential resistance in the circled region in each configuration.

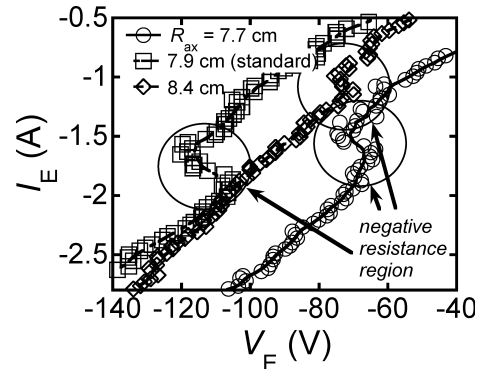


Fig. 3 The relation between bias voltage V_E and electrode current I_E . I_E show *s-shape* curves for V_E . I_E bifurcates for V_E with multiple solutions in the circled regions.

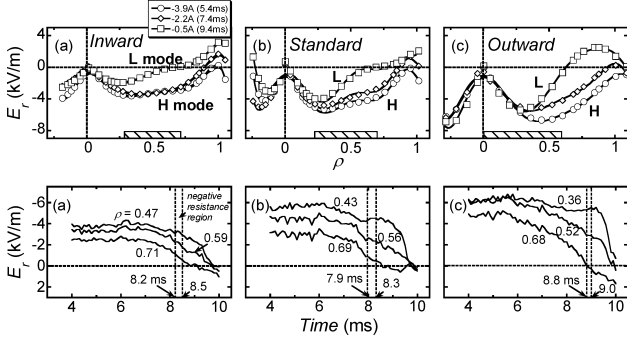


Fig. 4 The profiles and time evolutions of E_r for the configuration of (a) $R_{ax} = 7.7$ cm, (b) 7.9 cm, and (c) 8.4 cm. As seen in time evolutions, the steeper gradient region shifts to the inner region with $-I_E$ decreasing in each configuration. Thus, E_r collapses from the outer to the inner region. The strong E_r is maintained in the inner region even after transition to the L mode.

L mode. It is understood from both E_r profiles and time evolutions that the strong E_r is maintained in the inner region even after transition to the L mode.

4. Comparison with neoclassical theory

Neoclassical theory predicts the existence of a local maximum, which has an influence on sudden transition phenomena, in the ion viscosity for poloidal rotation. This is one of the characteristics of the L-H transition. To investigate the influence of ion viscosity on the L-H transition, the estimated poloidal ion viscosity was compared with the viscosity calculated from neoclassical theory. The poloidal driving force is balanced with a poloidal ion damping force, which consists of the poloidal ion viscosity term and a friction term caused by charge exchange. In the steady state, the normalised poloidal momentum balance equation for the ion [10,17], where the Shaing model [10,12,13] is applied to the ion viscosity, can be written as:

$$\begin{aligned} \frac{2}{\sqrt{\pi}} \frac{\langle r \rangle}{p_i} \langle J_\rho \rangle B_0 \\ = -\Pi_{p,n} - \frac{4}{\sqrt{\pi}} (1 + 2q^2) \frac{v_{in}}{(v_i / \langle r \rangle)} \Theta M_p, \end{aligned} \quad (1)$$

$$\Pi_{p,n} = \frac{4}{\sqrt{\pi}} \frac{\langle \mathbf{B}_p \cdot \nabla \cdot \mathbf{\Pi}_i \rangle}{n_i m_i v_i^2 (B_0 / q R_0)}, \quad (2)$$

$$M_p = -\frac{(E_p / B_0)}{\Theta v_i}, \quad \Theta = \frac{\varepsilon}{q}, \quad (3)$$

where angled brackets denote the flux surface average, J_ρ is the radial current density, B_0 is the magnetic field on the axis, n_i is the ion density, m_i is the mass of the ion, v_i is the ion thermal velocity, r is the minor radius, q is the safety factor, v_{in} is collision frequency between the ion and the neutral particle, M_p is the poloidal Mach number, \mathbf{B}_p is the poloidal magnetic field, $\mathbf{\Pi}_i$ is the ion viscous stress tensor, R_0 is the major radius, and $\varepsilon = \langle r \rangle / R_0$ is the toroidal ripple. The left side of Eq. (1) indicates the poloidal driving force of $\mathbf{J} \times \mathbf{B}$.

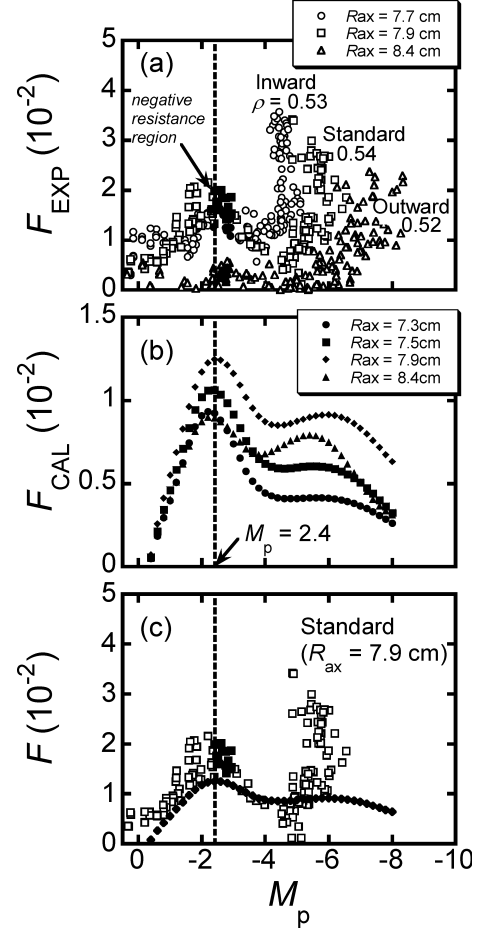


Fig. 5 The dependence of the ion viscosity on poloidal Mach number. (a) Experimental ion viscosity evaluated from poloidal driving force, (b) calculated ion viscosity applied to the Shaing model, and (c) the comparison between the experiment and the calculation for the standard configuration.

The electric current density is estimated as:

$$\langle J_\rho \rangle = \frac{I_E}{2\pi \langle r \rangle L}, \quad (4)$$

where L is the length of the magnetic axis. On the other hand, the right side of Eq. (1) indicates the poloidal ion damping force; the first term is the neoclassical ion viscous force and the second is the friction between the ion and the neutral particle. The collision frequency in the friction term can be written as:

$$v_{in} = \langle \sigma_{cx} u_i \rangle n_n, \quad (5)$$

where σ_{cx} is the cross-section of the charge exchange between the ion and a neutral particle [18,19], u_i is the velocity of the ion, and n_n is the density of the neutral particle.

Figure 5 shows the dependence of ion viscosity on M_p : (a) experimental ion viscous force F_{EXP} (the difference between the left side of Eq. (1) and the second term on the right side) for the configurations of $R_{ax} = 7.7$ cm (open circles), 7.9 cm (open squares), 8.4 cm (open triangles), and the closed symbols correspond to those in the region where

the plasma shows negative differential resistance; (b) calculated ion viscous force F_{CAL} , which is applied to the Shaing model (the first term on the right side of Eq. (1)) for the configurations of $R_{ax} = 7.3$ cm (closed circles), 7.5 cm (closed squares), 7.9 cm (closed diamonds), 8.4 cm (closed triangles); and (c) comparison between experiment and calculation for the standard configuration. In each configuration, the experimental driving force was estimated using the parameters measured at $\rho \sim 0.5$, and ion temperature T_i was assumed to be $0.2T_e$. On the other hand, the theoretical ion viscosity was calculated under the following conditions; the ratio of the collision frequency to bounce frequency for trapped particle, ∇p drift velocity to v_i , and the ∇T drift velocity to v_i were assumed to be 36, 0.36, and -0.093 , respectively, and T_i was assumed to be $0.6T_e$. As shown in Fig. 5, the dependence of experimental ion viscous force on M_p shows good agreement with the neoclassical theory. As shown in Fig. 5(a), the experimental ion viscosity has a local maximum at $M_p \sim -2.4$, where the plasma shows negative differential resistance in each configuration. This indicates that L-H transition occurs when the poloidal driving force exceeds a critical value as the local maximum of ion viscosity. The result agrees with the scenario of transition to H mode predicted by neoclassical theory. In the calculation (Fig. 5(b)), a local maximum also exists at $M_p \sim -2.4$ where there is a local maximum of estimated ion viscosity. As can be seen in Fig. 5(c), the dependence of experimental ion viscous force on M_p shows good agreement in $|M_p| < 4$ with the neoclassical theory in the standard configuration. The difference in $|M_p| > 4$ between the experiment and the neoclassical theory was thought to be due to ambiguity with regard to evaluation of the friction term. In this paper, friction was evaluated under the assumption that $T_i = 4$ eV and that it has a linear dependence on M_p . However, it is nonlinearly dependent on M_p in practice because the ion temperature and the cross-section of the charge exchange are changed with changes in electrode current. In the high M_p region where the plasma confinement state is H mode, plasma pressure and electron density increase such that the interaction between ions and neutral particles increases. Consequently, the value of friction was thought to be larger than the subtracted value.

Figure 6 shows the dependence of critical ion viscosity for L-H transition on configuration. The critical ion viscosity evaluated from the experiment corresponds to that in the negative differential region and the calculated value corresponds to that at $M_p = -2.4$. The value of critical ion viscosity is greatest in the standard configuration and lowest in outward configuration in both the experiment and calculation. The reason for the decrease in ion viscous force in the outward configuration can be explained qualitatively from the viewpoint of a ripple in the magnetic field and/or the shape of the magnetic surface. As shown in Table 1, toroidicity ε_{10} and helicity ε_{11} decrease with the shift in position of the magnetic axis to the outward configuration. Thus, the magnetic structure in the outward configuration has good poloidal symmetry. Therefore, the ion viscous force

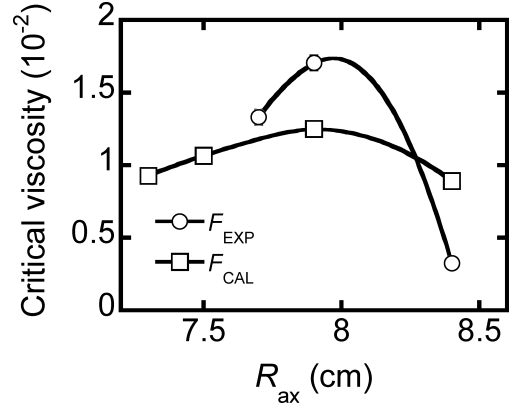


Fig. 6 The configuration effect on poloidal ion viscosity required for L-H transition. The circles are F_{EXP} and the squares are F_{CAL} . The critical ion viscosity is the largest in the configuration of $R_{ax} = 7.9$ cm in both the experiment and the calculation.

decreases because it is correlated with the amplitude of the magnetic field ripple. The bend in the magnetic surface in the outward configuration is less sharp than the other two at $\theta = 90^\circ$ and 270° as shown in Fig. 1. The plasma is thought to rotate easily for the poloidal direction and this is consistent with the lower poloidal ion viscosity.

The mechanism of L-H transition in TU-Helicac is the bifurcation phenomenon arising from the local maximum in the ion viscosity for poloidal flow velocity, and it can be explained by the neoclassical theory. The experiment showed good agreement with neoclassical theory. However, there were slight differences between the experimental and calculated values for the absolute ion viscosity. There are several possible explanations for this as follows: (i) The ion temperature was not measured. In this paper, the ion temperature was assumed to be $T_i = 0.2T_e$. However, the ion temperature should be measured for more quantitative evaluation of ion viscous force because ion viscosity and poloidal Mach number are proportional to T_i^{-1} and $T_i^{-1/2}$, respectively. (ii) The evaluated friction includes ambiguity of T_i and cross-section. For evaluation of friction, measurement of the ion temperature is also required. The friction must show nonlinear dependence on M_p as discussed above. (iii) The experimental ion viscosity might include the effect of anomalous viscosity. However, anomalous viscosity is not governed by ion viscosity because ion temperature is very low as $T_i \sim 4$ eV in TU-Helicac. (iv) Finally, the poloidal driving force does not correspond perfectly to the changes in local plasma parameters. However, the poloidal driving force and the poloidal Mach number were evaluated by plasma parameters measured locally using a Langmuir probe, the driving force also includes the electrode current as a global plasma parameter. Consequently, the driving force is averaged as a whole.

5. Summary

The hot-cathode-biasing experiment with three types of magnetic configuration in TU-Helicac yielded the following

findings: (i) Plasmas show negative resistance after transition from the H mode to the L mode in all configurations. (ii) The radial electric field collapses from the outer to the inner region with transition from the H mode to the L mode. (iii) The poloidal ion viscosity estimated from the experiment shows good agreement with neoclassical theory in $|M_p| < 4$. (iv) The poloidal ion viscosities estimated from the experiments have local maxima at $M_p \sim -2.4$ in all configurations studied here. (v) The poloidal ion viscosities at local maximum correspond to those in the negative differential resistance region. (vi) The regions where the local maximum of ion viscosity exists agree with the predictions from neoclassical theory. (vii) In both experiment and calculation, the value of the local maximum of the ion viscosity is largest in the standard configuration.

Acknowledgment

Authors wish to acknowledge Prof. K. Itoh for useful discussion. This work was supported in part by the LHD Joint Planning Research program at National Institute for Fusion Science.

References

- [1] F. Wagner, G. Becker *et al.*, Phys. Rev. Lett. **49**, 1408 (1982).
- [2] K.H. Burrell *et al.*, Phys. Rev. Lett. **59**, 1432 (1987).
- [3] M. Kotschenreuther *et al.*, Phys. Plasmas **2**, 2381 (1995).
- [4] V. Erckmann *et al.*, Phys. Rev. Lett. **70**, 2086 (1993).
- [5] K. Toi *et al.*, Plasma Phys. Control. Fusion **38**, 1289 (1996).
- [6] S. Inagaki *et al.*, Jpn. J. Appl. Phys. **36**, 3697 (1997).
- [7] S. Kitajima *et al.*, Int. J. Appl. Electromagnetics and Mechanics **13**, 381 (2002).
- [8] S. Kitajima *et al.*, IEEE Conference Record of 2003 IEEE International Conference on Plasma Science, 465 (2003).
- [9] K.C. Shaing *et al.*, Phys. Fluids B **2**, 1492 (1990).
- [10] K.C. Shaing and E.C. Crume, Jr., Phys. Rev. Lett. **63**, 2369 (1989).
- [11] S.-I. Itoh and K. Itoh, Nucl. Fusion **29**, 1031 (1989).
- [12] K.C. Shaing, Phys. Fluids B **5**, 3841 (1993).
- [13] M. Yokoyama, N. Nakajima and M. Okamoto, NIFS-519 (1997).
- [14] S. Kitajima *et al.*, Jpn. J. Appl. Phys. **30**, 2606 (1991).
- [15] T. Zama *et al.*, Jpn. J. Appl. Phys. **32**, 349 (1993).
- [16] S. Kitajima *et al.*, Jpn. J. Appl. Phys. **36**, 4223 (1995).
- [17] V. Rozhansky and M. Tendler, Phys. Fluids B **2**, 1877 (1992).
- [18] J. Cornelis *et al.*, Nucl. Fusion **34**, 171 (1994).
- [19] C.F. Barnett, ed., *COLLISIONS of H, H2, He and Li ATOMS and IONS with ATOMS and MOLECULES*, ORNL-6086, Vol. 1, A-72, OAK RIDGE NATIONAL LABORATORY, Office of Fusion Energy, U. S. Department of Energy.